Drift

By M. J. LIGHTHILL
Department of Mathematics, University of Manchester

(*Received* 12 *December* 1955)

Summary

Sir Charles Darwin has advocated a study of the 'drift' of material surfaces in the classically investigated irrotational flows past bodies. This suggestion is followed up and given further support in the present paper. In particular, it is shown how secondary flows can be evaluated by use of the 'drift function' t for the primary flow. This is a function (§ 1) such that material surfaces initially at right angles to the stream drift into shapes expressible by equations $t =$ constant.

The analysis leads to a simple expression (§ 4) for the secondary velocity field in the flow past an infinite cylinder of any cross-section, with the upstream velocity normal to its axis and increasing linearly with distance along the axis—a problem in which only the secondary vorticity field was previously known. The drift past a sphere is computed and illustrated (§ 6), and the secondary vorticity field in shear flow past a sphere is tabulated (§ 7). There is also a detailed study (§ 3) of the asymptotic form of the secondary velocity field in flow past any body, based on a result of Darwin concerning 'hydrodynamic mass'.

1. Introduction

Sir Charles Darwin (1953) has shown what interesting and important conclusions can be drawn by studying the deformation, or 'drift' as he calls it, of material surfaces—and, generally, by studying the motions of individual particles—in the classical problems of irrotational flow of fluid about bodies. Some more advantages of this approach are indicated in the present paper. In particular, the Cauchy–Helmholtz–Kelvin result that vortex lines move with the fluid, while the magnitude of the vorticity changes in proportion to the local stretching of the vortex lines, is combined with it to deduce how the vorticity in a weakly-sheared flow is altered in the presence of an obstacle, as a result of deformation of vortex lines by the irrotational component of the flow about the obstacle.

Detailed results are obtained for the sphere, which Darwin (1953) treated only briefly. The deduced vorticity field in shear flow past a sphere (§ 7) will be used in a later paper, together with the recent derivation (Lighthill 1956) of the image system of a vortex element in a sphere, to compute certain features of the secondary flow, and in particular the upstream displacement of the stagnation streamline—a quantity related to the 'displacement of the effective centre' of pitot tubes in shear flow, described by Young & Maas (1936).

The approach leads also (§ 4) to a convenient expression for the secondary velocity field in the flow past an infinite cylinder of any cross-section with the upstream velocity normal to its axis and increasing linearly with distance along the axis; in this problem, only the secondary vorticity was previously known (Hawthorne 1954).

Hydrodynamics has achieved impressive results by the simplification of concentrating on the steady (or nearly steady) field of flow velocities relative to a moving body, as specified in the Eulerian manner. This does not mean, however, that additional information, regarding the history of individual particles of fluid, is of no value. For example, Darwin (1953) shows that, when a circular cylinder moves through otherwise undisturbed fluid, a typical fluid particle begins to move forwards before the body reaches it, then starts to move outwards (away from the path of the body) and forwards, then outwards and backwards, and is moving backwards (parallel to the path of the body but in the opposite sense) when the body is abreast of it; it then moves inwards and backwards, inwards and forwards, and finally comes to rest while moving forwards, at a point slightly ahead of its original position. This result throws light on the familiar gyrations of the air, and of small particles suspended in it, when any large body moves past.

Darwin considers also "an infinite thin plane of fluid, at right angles to the motion, marked so as to be made recognizable, perhaps by means of some dye-stuff", and asks "after the passage of the body, what is the form assumed by this infinite plane ?". The answer is that the part near where the body has been has drifted *forwards*, and that the fluid between the initial and final positions of the material surface has a mass equal to the 'hydrodynamic' or 'virtual' mass associated with the body's motion.

It could, perhaps, have been expected that the hydrodynamic mass would equal the net 'mass movement' (integral of momentum with respect to time) induced in the fluid per unit distance travelled by the body, so that the total mass movement per unit distance equals the mass of the body plus the hydrodynamic mass. However, the study of hydrodynamic mass from an Eulerian point of view had left this interpretation hidden until Darwin discovered it.

It should be emphasized that no abandonment of the Eulerian steady velocity field is involved in the studies here described, nor is there any question of using the Lagrangian equations of motion. Rather it is necessary to determine, not only the streamlines, but also on each streamline the *time* at which a fluid particle reaches any given point, measured from some fixed time for the particle—say, from when it passes across a particular plane at right angles to the undisturbed stream (as in Darwin 1953), or (as in the present paper) from when it *would* have passed across a particular plane had the stream remained undisturbed. Thus, if the latter plane is $x=0$, then we require the solution of

$$dt = \frac{dx}{v_x} = \frac{dy}{v_y} = \frac{dz}{v_z} \quad \text{with } t - \frac{x}{U} \to 0 \text{ as } x \to -\infty \tag{1}$$

(where v_x is the x-component of velocity, etc., and the undisturbed stream has $v_x = U, v_y = v_z = 0$). The advantage of this definition over Darwin's is that, far upstream, material planes at right angles to the stream are planes $t = \text{constant}$; hence the surfaces into which these are deformed, in which we are particularly interested, are all given by $t = \text{constant}$.

It is easy, in terms of this 'drift function' t, to determine how vortex lines, initially at right angles to the stream, are deformed and stretched by the irrotational flow about the body (here, the vortex lines are supposed weak enough for the additional stretching by the secondary flow due to their presence to be neglected). A vortex element joining a pair of points on two neighbouring streamlines will always join points on these two streamlines, and they will always be points with the same value of t. The vector separation of these two points, divided by the scalar separation of the original pair, gives the direction and magnitude of the vorticity divided by its upstream magnitude. The details come out simply once the drift function t is known.

The work is carried out in detail for a sphere, as being the three-dimensional shape for which (owing to the simplicity of the image system) the secondary flow has the best chance of being calculated. This secondary flow will be studied in detail in a later paper. Here, only its behaviour at large distances from the sphere is worked out, since this deduction does not depend on the details of the image system, but conversely leans heavily on Sir Charles Darwin's result concerning hydrodynamic mass. In fact, it is shown (§ 3) that, for any finite body so placed that the irrotational flow exerts no yawing moment on it, the part of the secondary velocity field which falls off like the inverse square of distance from the body has a simple form depending only on the hydrodynamic mass associated with the body's motion and on the mass of fluid displaced by the body.

Finally, it is pointed out that this secondary velocity field induces what might be called a 'tertiary' velocity field, which falls off like the inverse *first power* of the distance, and so on; the complete series for the remote influence of the obstacle is non-uniformly convergent, and the true behaviour which it represents is probably of a damped-wave type. The remote influence on a weakly-sheared oncoming flow of 'half-body' shapes like the Rankine source body is also discussed.

The method of this paper for calculating vorticity fields is an alternative to that developed by Hawthorne (1951, 1954) and Hawthorne & Martin (1955). Their integral for the streamwise component of vorticity is convenient for numerical computation but was found unsuitable for analytical estimation near singularities and at infinity. The present method is particularly suitable for this purpose, and gives all components of the vorticity with equal ease. Detailed comparison between the results of the two methods for the sphere is given in § 7. This has been made possible by Professor Hawthorne's kindness in putting at the author's disposal data additional to those in the papers cited.

One advantage of the present expressions for the secondary vorticity over those of Hawthorne (1954) accrues almost by chance. The form of these expressions, in the case of flow past an infinite cylinder, with the upstream velocity normal to its axis and increasing linearly with distance along the axis, is such that one can write down at once, by inspection, the secondary velocity field which the vorticity induces. This is done in § 4, and figure 1 shows the computed secondary flow for the case of a circular cylinder. This derivation of the secondary flow past cylinders appears somewhat as a sideline in this paper, but it may prove the most useful of the results which are obtained.

2. The vorticity field in weakly-sheared flow past an obstacle

Consider flow past an obstacle in which the velocity field far upstream is a parallel flow

$$v_x = V(y, z), \qquad v_y = v_z = 0. \tag{2}$$

Suppose that the obstacle is near the axis $y = z = 0$, and that $V(y, z)$ varies only a little from its value $V(0, 0) = U$ over a range of variation of y and z large compared with the size of the obstacle. A particularly interesting case is that in which the gradient of V also varies little over this range, so that with suitable choice of axes we can take

$$v_x = U + Ay, \qquad v_y = v_z = 0 \tag{3}$$

far upstream, for some rate of shear A.

In all cases, the irrotatonal flow about the obstacle with uniform upstream velocity U will be called the primary flow. The vortex lines, which far upstream lie in planes $x =$ constant, are deformed by the primary flow into shapes which will be calculated, after which (§ 3) the resulting secondary vorticity field and the asymptotic form of the associated secondary velocity field far from the obstacle will be deduced. The work is displayed only for the simple case (3), but results for the more general case (2) are quoted at the end of § 3.

Let the streamlines of the primary flow be represented by equations of the form

$$y = y(x, y_0, z_0), \qquad z = z(x, y_0, z_0), \tag{4}$$

where

$$y_0 = \lim_{x \to -\infty} (y), \qquad z_0 = \lim_{x \to -\infty} (z). \tag{5}$$

Thus expressions (4) are solutions of equations (1) for y and z, and can be supposed obtained by the ordinary methods of hydrodynamics. Then the solution for the additional variable t is

$$t = t(x, y_0, z_0) = \frac{x}{U} + \int_{-\infty}^{x} \left\{ \frac{1}{v_x(x, y_0, z_0)} - \frac{1}{U} \right\} dx, \tag{6}$$

where $v_x(x, y_0, z_0)$ signifies the value of the velocity component v_x at the point x on the streamline given by (4).

In case (3) the upstream vorticity field is given by

$$\omega_x = \omega_y = 0, \qquad \omega_z = -A, \tag{7}$$

so that the vortex lines are parallel to the z-axis. An element of vortex line stretching from (X, y_0, z_0) to $(X, y_0, z_0 + \delta z_0)$, where X is large and negative, is deformed by the primary flow, but always remains on a surface $t=$ constant and joins points on the streamlines specified by y_0, z_0 and y_0, $z_0+\delta z_0$. When its length is δr, the vorticity is changed from its initial value $-A$ to $-A\delta r/\delta z_0$, and its direction lies along the new position of the element. Its components are therefore

$$\boldsymbol{\omega}=-A\left\{\left(\frac{\partial x}{\partial z_0}\right)_{t,y_0},\ \left(\frac{\partial y}{\partial z_0}\right)_{t,y_0},\ \left(\frac{\partial z}{\partial z_0}\right)_{t,y_0}\right\},\tag{8}$$

where the suffixes indicate the variables to be kept constant in each differential coefficient.

Now by (6),
$$dt=\frac{\partial t}{\partial x}dx+\frac{\partial t}{\partial y_0}dy_0+\frac{\partial t}{\partial z_0}dz_0,\tag{9}$$

so that
$$\left(\frac{\partial x}{\partial z_0}\right)_{t,y_0}=-\frac{\partial t/\partial z_0}{\partial t/\partial x}=-v_x\frac{\partial t}{\partial z_0}.\tag{10}$$

We have also
$$\left(\frac{\partial y}{\partial z_0}\right)_{t,y_0}=\left(\frac{\partial y}{\partial z_0}\right)_{x,y_0}+\left(\frac{\partial y}{\partial y}\right)_{y_0,z_0}\left(\frac{\partial x}{\partial z_0}\right)_{t,y_0}$$
$$=\left(\frac{\partial y}{\partial z_0}\right)_{x,y_0}+\frac{v_y}{v_x}\left(-v_x\frac{\partial t}{\partial z_0}\right),\tag{11}$$

which, with a similar result for $\partial z/\partial z_0$, gives by (8)

$$\omega_x=Av_x\frac{\partial t}{\partial z_0},\quad \omega_y=Av_y\frac{\partial t}{\partial z_0}-A\frac{\partial y}{\partial z_0},\quad \omega_z=Av_z\frac{\partial t}{\partial z_0}-A\frac{\partial z}{\partial z_0}.\tag{12}$$

Far downstream of the obstacle, we have

$$v_x\to U,\qquad v_y\to 0,\qquad v_z\to 0,\qquad t-\frac{x}{U}\to\frac{1}{U}X(y,z),\tag{13}$$

where $X(y, z)$ is Darwin's 'total drift,' the ultimate displacement of a particle of fluid (relative to particles in its plane which are far from the path of the obstacle). We shall need Darwin's result

$$\int_{-\infty}^{\infty}\int_{-\infty}^{\infty}X(y,z)\,dydz=V_h,\tag{14}$$

where V_h is the volume of fluid whose mass is the 'hydrodynamic mass' associated with the body's motion.

In the limiting conditions (13), the vorticity components (12) satisfy

$$\omega_x\to A\frac{\partial X}{\partial z},\qquad \omega_y\to 0,\qquad \omega_z\to -A,\tag{15}$$

so that the only new component far downstream is ω_x, which Hawthorne calls the 'secondary trailing vorticity'.

If the primary flow has a velocity potential $U(x+\phi)$, so that ϕ is the 'disturbance potential', there is a useful approximation to the solutions (4) and (6) of equations (1), which is valid on any streamline that remains far from the obstacle (so that $(v_x-U)/U=\partial\phi/\partial x\ll 1$ all along it). Such a streamline takes the form $y\doteqdot y_0$, $z\doteqdot z_0$ to a first approximation, and to a second approximation

$$y\doteqdot y_0+\int_{-\infty}^{x}\frac{\partial\phi}{\partial y}dx,\qquad z\doteqdot z_0+\int_{-\infty}^{x}\frac{\partial\phi}{\partial z}dx,\tag{16}$$

while equation (6) becomes

$$t = \frac{x}{U} - \int_{-\infty}^{x} \frac{1}{U}\left\{\frac{\partial\phi/\partial x}{1+\partial\phi/\partial x}\right\} dx \doteqdot \frac{x-\phi}{U}. \tag{17}$$

Note that the integrals in (16) and (17) need not be taken along the streamlines; to the approximation involved, y and z may be taken constant therein, and equal either to y_0 and z_0 or to their values at the point under consideration.

Substituting from (16) and (17) in (12), we obtain to the same approximation

$$\omega_x \doteqdot -A\frac{\partial\phi}{\partial z}, \qquad \omega_y \doteqdot -A\int_{-\infty}^{x} \frac{\partial^2\phi}{\partial y \partial z} dx, \qquad \omega_z + A \doteqdot -A\int_{-\infty}^{x} \frac{\partial^2\phi}{\partial z^2} dx. \tag{18}$$

Equations (18) are valid far from the body, except downstream of it on streamlines which have not *remained* far from the body. On these, in fact, (15) holds.

3. The secondary flow in weakly-sheared flow past an obstacle

The secondary flow associated with the secondary vorticity field is calculated in three parts:

(i) a part, which is the gradient of a potential ϕ_1 vanishing at infinity, and whose normal velocity component on the body surface cancels that due to the shear flow $v_x = Ay$, $v_y = v_z = 0$ which results from the undisturbed vorticity distribution $(0, 0, -A)$;

(ii) the Biot–Savart velocity field, say $\mathbf{v}_1$, of the vorticity *change* $\boldsymbol{\omega}_1 = (\omega_x, \omega_y, \omega_z + A)$; note that the Biot–Savart integral would not converge if the undisturbed vorticity field were not subtracted out;

(iii) a further irrotational part, which is the gradient of a potential ϕ_2 vanishing at infinity, and whose normal velocity component on the body surface cancels that due to (ii); this may be regarded as the velocity field of the image vorticity associated with $\boldsymbol{\omega}_1$, while part (i) is that of the image vorticity associated with the undisturbed vorticity field.

Now, by general properties of harmonic functions, the irrotational velocity fields (i) and (iii) fall off like the inverse cube of the distance from the body, because the required normal velocity on the surface has a zero integral over the surface in each case (so that in 'Green's equivalent layer' the total source strength is zero). However, the Biot–Savart field (ii) falls off more slowly, and its asymptotic form will now be derived.

First, we see by inspection that a velocity field corresponding to the asymptotic form (18) of the vorticity change $\boldsymbol{\omega}_1$ is

$$v_x = -A\int_{-\infty}^{x} \frac{\partial\phi}{\partial y} dx, \qquad v_y = A\phi, \qquad v_z = 0. \tag{19}$$

(Its curl is (18), and its divergence vanishes). Since the disturbance potential ϕ for flow past any finite body is asymptotically that of a doublet, this velocity field (19) falls off like the inverse square of the distance from the body, more slowly than that of (i) and (iii) above.

Next, if $\boldsymbol{\omega}_2$ is the difference of the vorticity change $\boldsymbol{\omega}_1$ from its asymptotic form (18), and $\mathbf{v}_2$ is its associated (Biot–Savart) velocity field, $\mathbf{v}_2$ can be expressed asymptotically as the velocity field of a single vortex element of strength equal to the total strength of the field $\boldsymbol{\omega}_2$, thus

$$\mathbf{v}_2 \sim \frac{1}{4\pi}\left(\int \boldsymbol{\omega}_2\, d\tau\right) \wedge \nabla\left(\frac{1}{r}\right), \tag{20}$$

where $r=\sqrt{(x^2+y^2+z^2)}$ and the integral is over the whole region occupied by the fluid. This step is permissible only after the inverse-cube part of $\boldsymbol{\omega}_1$ has been subtracted out, as the integral would otherwise be only semi-convergent.*

Now $\int \boldsymbol{\omega}_2\, d\tau$ does not vanish, because of the trailing vorticity. If the integral is taken over a large rectangular box, we have

$$\begin{aligned}\int_V \boldsymbol{\omega}_2\, d\tau &= \int_V \{\operatorname{div}(x\boldsymbol{\omega}_2),\ \operatorname{div}(y\boldsymbol{\omega}_2),\ \operatorname{div}(z\boldsymbol{\omega}_2)\}d\tau \\ &= \int_S (x, y, z)\boldsymbol{\omega}_2\cdot\mathbf{n}\, dS \\ &= \int_{-\infty}^{\infty}\int_{-\infty}^{\infty} (x,y,z)A\frac{\partial X}{\partial z}\, dydz \\ &= (0, 0, -AV_h),\end{aligned} \tag{21}$$

where (15) and Darwin's result (14) have been used. Note that only the rear face of the box contributes to $\int_S$ because the part of $\boldsymbol{\omega}_1$ which falls off like $1/r^3$ has been taken out. By (20) and (21),

$$\mathbf{v}_2 \sim \frac{AV_h}{4\pi}\left(-\frac{y}{r^3},\ \frac{x}{r^3},\ 0\right) \quad \text{as } r \to \infty. \tag{22}$$

Now, for a body so placed that the irrotational flow exerts no yawing moment on it, the asymptotic behaviour of the disturbance potential (Taylor 1928) is

$$\phi \sim \frac{(V_b+V_h)x}{4\pi r^3}, \tag{23}$$

where V_b is the volume of the body. Hence, for such a body, combining the results (19) and (22), we obtain

$$\mathbf{v}_1 \sim \frac{A(V_b+2V_h)}{4\pi}\left(-\frac{y}{r^3},\ \frac{x}{r^3},\ 0\right). \tag{24}$$

More generally, ϕ contains terms in y/r^3 and z/r^3 proportional to the moments on the body, about the z-axis and y-axis respectively, and these make an additional contribution, through (19), to (24). It may be noted, however, that they do not affect the value of v_{1y} on $y=z=0$, which alone influences the first-order displacement of the stagnation streamline.

* As a matter of interest, if this argument is incorrectly applied to the inverse-cube part of $\boldsymbol{\omega}$, it gives an asymptotic contribution to the velocity field from this part only two-thirds as much as the true contribution (19).

It has been seen that a primary flow with the disturbance velocities falling off like r^{-3} produces secondary flow velocities falling off like r^{-2}. It may be questioned whether this conclusion does not undermine itself, since the assumption that the disturbance velocities are asymptotically given by a potential (23) is used to derive (24). However, the process by which (24) was derived from (23) was a linear one, so that the existence of a further contribution (24) to the disturbance velocities at infinity merely makes an additional (call it 'tertiary') contribution to the vorticity field and the resulting velocity field. Calculations (along lines similar to those above) show that the asymptotic form of the tertiary velocity field is of order r^{-1}, being in fact

$$v_x = \frac{A^2(V_b+2V_h)(x^2+y^2)}{8\pi U r^3},$$

$$\frac{v_y}{y} = \frac{v_z}{z} = \frac{A^2(V_b+2V_h)}{8\pi U}\left\{\frac{(z^2-y^2)(1+x/r)}{(y^2+z^2)^2} + \frac{xz^2}{(y^2+z^2)r^3}\right\}, \tag{25}$$

at all points far from the body except those immediately downstream of it.

It is obvious that the series for the disturbance velocity whose first three terms are given by the primary flow $U\nabla\phi$, the secondary flow (24) and the tertiary flow (25), is of little value at distances from the body comparable with U/A. In this region, where the disturbances are very small, a truer picture may be obtained by solutions of the linearized form

$$U\frac{\partial}{\partial x}\operatorname{curl}\mathbf{v} = -A\frac{\partial \mathbf{v}}{\partial z} \tag{26}$$

of Helmholtz's equation for the vorticity. Solutions of (26) which tend to zero at large distances are usually wavy, for example

$$\mathbf{v} \sim \mathbf{v}_0 r^{-n}\exp[i(ax+by+cz)A/U], \tag{27}$$

where a, b, c are numbers satisfying $c^2 = a^2(a^2+b^2+c^2)$. Evidently (27) expanded in powers of A/U would give a series of the kind described above, but its convergence would be non-uniform for r large, and the true order of magnitude of the whole is no greater than that of the first term.

The above gives a mathematical reason for not feeling alarmed at the orders of magnitude found. Physically, one would not expect the approximation to be good at distances from the body comparable with that at which the oncoming flow differs from the primary flow by an amount equal to itself.

We consider next how the results are to be modified if a body experiences drag, so that the irrotational flow outside the wake has a source-like behaviour at infinity (corresponding to the reduced mass flow in the wake). The same problem arises for 'half-bodies' extending to infinity downstream—such as pitot tubes—which exhibit the same source-flow behaviour. In either case the disturbance potential satisfies

$$\phi \sim -\frac{m}{4\pi r} \quad \text{as } r \to \infty, \tag{28}$$

where, for a finite body with a wake, m is the drag divided by ρU^2, while, for irrotational flow about a half-body, m is the cross-sectional area of the semi-infinite cylindrical portion. By (19), the secondary flow then is asymptotically

$$v_x = -\frac{Amx}{y^2+z^2}\left(1+\frac{x}{r}\right), \qquad v_y = -\frac{Am}{4\pi r}, \qquad v_z = 0, \tag{29}$$

far from the body except immediately downstream of it. The contribution of the Biot–Savart field of $\boldsymbol{\omega}_2$ falls off like r^{-2} and so does not have to be included in (29). As with (24), (29) is probably only a term in a series whose early terms are a poor approximation for values of r comparable with U/A.

Finally, we give without proof some results for the general case of a parallel flow given by equations (2) far upstream. The secondary vorticity field is

$$\omega_x = v_x \frac{\partial(V_0, t)}{\partial(y_0, z_0)}, \qquad \omega_y = v_y \frac{\partial(V_0, t)}{\partial(y_0, z_0)} - \frac{\partial(V_0, y)}{\partial(y_0, z_0)},$$

$$\omega_z = v_z \frac{\partial(V_0, t)}{\partial(y_0, z_0)} - \frac{\partial(V_0, z)}{\partial(y_0, z_0)}, \tag{30}$$

where V_0 stands for $V(y_0, z_0)$ and the notation for Jacobians has been used. The secondary trailing vorticity is

$$\lim_{x\to+\infty} (\omega_x) = \frac{\partial(V, X)}{\partial(y, z)}. \tag{31}$$

The asymptotic form of the vorticity change $\boldsymbol{\omega}_1$, as $r\to\infty$ except immediately behind the body (corresponding to (18), is

$$\boldsymbol{\omega}_1 = \left(\omega_x, \omega_y - \frac{\partial V}{\partial z}, \omega_z + \frac{\partial V}{\partial y}\right)$$

$$\sim \left\{ \frac{\partial(\phi, V)}{\partial(y, z)}, \frac{\partial\left(\int_{-\infty}^{x} \frac{\partial\phi}{\partial y} dx, V\right)}{\partial(y, z)} - \frac{\partial^2 V}{\partial z^2}\int_{-\infty}^{x} \frac{\partial\phi}{\partial z} dx - \frac{\partial^2 V}{\partial y \partial z}\int_{-\infty}^{x} \frac{\partial\phi}{\partial y} dx, \right.$$

$$\left. \frac{\partial\left(\int_{-\infty}^{x} \frac{\partial\phi}{\partial z} dx, V\right)}{\partial(y, z)} + \frac{\partial^2 V}{\partial y \partial z}\int_{-\infty}^{x} \frac{\partial\phi}{\partial z} dx + \frac{\partial^2 V}{\partial y^2}\int_{-\infty}^{x} \frac{\partial\phi}{\partial y} dx \right\}. \tag{32}$$

The asymptotic velocity field $\mathbf{v}_1$ corresponding to (32) is less simple than one would like, because the expression analogous to (19), namely

$$\left(-\frac{\partial V}{\partial y}\int_{-\infty}^{x} \frac{\partial\phi}{\partial y} dx - \frac{\partial V}{\partial z}\int_{-\infty}^{x} \frac{\partial\phi}{\partial z} dx, \frac{\partial V}{\partial y}\phi, \frac{\partial V}{\partial z}\phi\right), \tag{33}$$

although it has a curl equal to (32), is not solenoidal unless $\partial^2 V/\partial y^2 + \partial^2 V/\partial z^2 = 0$. In general, then, $\mathbf{v}_1$ is asymptotically (33) minus grad ψ, where $\nabla^2\psi = \phi\nabla^2 V$.

As in the special case, the secondary flow is asymptotically $\mathbf{v}_1 + \mathbf{v}_2$, where $\mathbf{v}_2$ is the velocity field of a single vortex element of strength equal to the total strength of the field $\boldsymbol{\omega}_2$. We can show that

$$v_2 \sim \frac{1}{4\pi}\left(\int_{-\infty}^{\infty}\int_{-\infty}^{\infty} \frac{\partial V}{\partial z} X \, dydz\right)\left(-\frac{z}{r^3}, 0, \frac{x}{r^3}\right)$$

$$+ \frac{1}{4\pi}\left(\int_{-\infty}^{\infty}\int_{-\infty}^{\infty} \frac{\partial V}{\partial y} X \, dydz\right)\left(-\frac{y}{r^3}, \frac{x}{r^3}, 0\right), \tag{34}$$

where each integral can be interpreted as the product of V_h (see (14)) and a mean shear over a region comparable with the body size.

4. Theory for two-dimensional primary flows

The theory for a uniformly sheared oncoming flow (3) will now be specialized further to the case of a two-dimensional primary flow in the (x,z)-plane about a cylinder with generators in the y-direction. (Note that the assumed oncoming vorticity (7) is entirely in the z-direction, but that the theory can be trivially extended to cases where there is in addition some uniform oncoming vorticity in the y-direction, since vortex elements in that direction are not stretched at all by the primary flow.) The case in question is remarkable in that the exact secondary flow can be calculated.

The streamlines of the primary flow may be written

$$y=y_0; \qquad z=z(x, z_0), \tag{35}$$

and the time t (see (6)) is a function of x and z_0 alone, giving, by (12), vorticity components in the form

$$\omega_x = Av_x\frac{\partial t}{\partial z_0}, \qquad \omega_y=0, \qquad \omega_z = Av_z\frac{\partial t}{\partial z_0} - \frac{\partial z}{\partial z_0}. \tag{36}$$

Some simplification is possible for these flows, however, if the time t, once calculated, is expressed as a function of x and z, rather than of x and z_0. Since Uz_0, by (5), is the stream function of the two-dimensional flow,

$$\frac{\partial z_0}{\partial z} = -\frac{v_z}{U}, \qquad \frac{\partial z_0}{\partial z} = \frac{v_x}{U}. \tag{37}$$

Using these results to transform (36) for the case when t is expressed as $t(x, z)$, we obtain

$$\omega_x = AU\frac{\partial t}{\partial z}, \qquad \omega_y=0, \qquad \omega_z = -AU\frac{\partial t}{\partial x}. \tag{38}$$

Thus the vorticity is simply proportional to grad t in magnitude, but is perpendicular to it in direction (as it must be because $t=$ constant along vortex lines). This result could also have been obtained by physical argument: the rate of stretching of the vortex elements on which $t=$ constant must be inversely proportional to the distance between successive lines $t=$ constant by conservation of mass.

The exact secondary flow can be deduced from (38) by inspection, in three parts (i), (ii) and (iii) as in § 3. The potential ϕ_1 whose gradient cancels out the normal component of the shear flow $(Ay, 0, 0)$ on the body is

$$\phi_1 = Ay\phi, \tag{39}$$

where $\phi(x,z)$ is the 'disturbance potential' as in §§ 2 and 3. The Biot–Savart field of the vorticity change

$$\boldsymbol{\omega}_1 = \left(AU\frac{\partial t}{\partial z}, 0, A-AU\frac{\partial t}{\partial x}\right) \tag{40}$$

is

$$v_x=0, \qquad v_y=A(x-Ut), \qquad v_z=0, \tag{41}$$

because the curl of (41) is (40) and its divergence vanishes. Finally, no extra irrotational portion (iii) is needed because the velocity field (41) is wholly tangential to the body.

Combining the secondary flows (39) and (41) with the primary flow and the oncoming shear flow, we see that the velocity components in any plane $y = \text{constant}$ are simply

$$v_x = (U + Ay)\left(1 + \frac{\partial\phi}{\partial x}\right), \qquad v_z = (U + Ay)\frac{\partial\phi}{\partial z}, \tag{42}$$

namely, the ordinary potential flow with the upstream velocity appropriate to that plane. Superimposed on these motions, however, is a flow parallel to the generators given by

$$v_y = A(x + \phi - Ut). \tag{43}$$

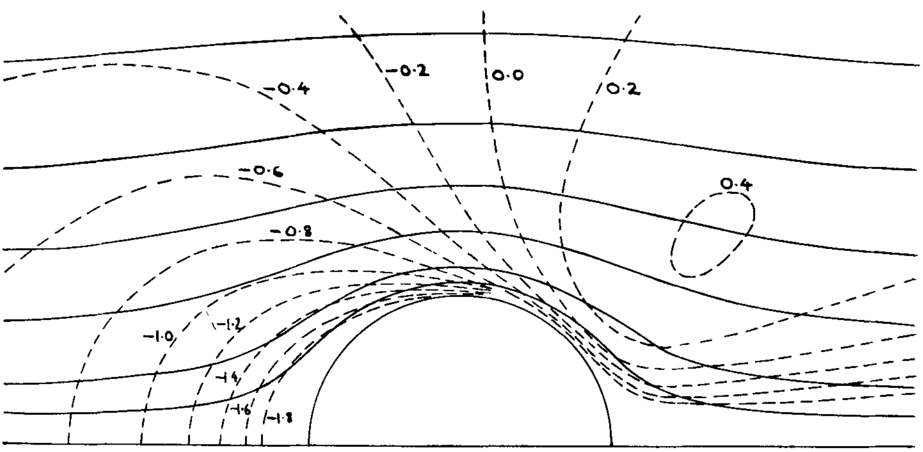

Figure 1. Primary and secondary flow about a circular cylinder of radius a, with axis the y-axis, when the upstream velocity is $(U+Ay, 0, 0)$.
———Streamlines of the primary flow (note that the velocity components in the x and z directions follow these streamlines even when the secondary flow is included).
– – – – –Contours of constant v_y/Aa (note that the negative values, which predominate, denote secondary flow in the direction of decreasing primary flow velocity). (Flow is from left to right and only the upper half is shown.)

As an example, figure 1 shows the distribution of v_y/Aa for sheared flow about a circular cylinder of radius a, computed from Sir Charles Darwin's evaluation of t for a circular cylinder. Remembering that the y-axis is along the axis of the cylinder in the direction of increasing velocity, we see that the greatest secondary flow velocities are in the direction of decreasing velocity—physically, because this is the direction of decreasing stagnation-point pressure. Like t itself, the secondary flow velocity has theoretically a logarithmic infinity on the surface of the body (and on the central streamline behind the body); but viscous resistance must place a practical limit on the velocities which can be achieved.

5. Theory for axisymmetrical primary flows

Some simplifications, analogous to those of § 4, are possible when the primary flow is axisymmetric, though unfortunately they do not extend so far as a simple exact solution for the secondary flow.

If x, ρ, λ are cylindrical polar coordinates relative to the axis of symmetry, the streamlines of the primary flow may be written

$$\rho = \rho(x, \rho_0), \quad \lambda = \text{constant}. \tag{44}$$

In ordinary hydrodynamics such streamlines are obtained in the form $\psi = \text{constant}$, where ψ is Stokes's stream function; note that the relation between ψ and $\rho_0 = \lim_{x \to \infty} (\rho)$ is

$$\psi = \tfrac{1}{2} U \rho_0^2. \tag{45}$$

The time
$$t = t(x, \rho_0) = \frac{x}{U} + \int_{-\infty}^{x} \left\{ \frac{1}{v_x(x, \rho_0)} - \frac{1}{U} \right\} dx \tag{46}$$
is independent of λ.

If ρ and λ are related to the coordinates x, y and z used in earlier sections by the equations $y = \rho \cos \lambda$, $z = \rho \sin \lambda$, then the upstream flow (3) and its associated vorticity field may be written

$$v_x = U + A\rho \cos \lambda, \quad v_\rho = v_\lambda = 0, \quad \omega_x = 0, \quad \omega_\rho = -A \sin \lambda, \quad \omega_\lambda = -A \cos \lambda. \tag{47}$$

The component ω_λ, the 'ring vorticity', varies in a particularly simple manner due to the stretching of vortex elements by the primary flow. An element of ring vorticity subtends always the same angle $\delta\lambda$ at the axis, and so its length varies in direct proportion to the radius ρ. At any point, therefore,

$$\omega_\lambda = (-A \cos \lambda) \frac{\rho}{\rho_0} = (-A \cos \lambda) \rho \sqrt{\left(\frac{U}{2\psi} \right)}, \tag{48}$$

where (45) has been used to throw the result into an alternative form involving Stokes's stream function.

The radial and axial components of vorticity, ω_r and ω_x, are stretched in a manner depending more closely on the details of the flow in planes $\lambda = \text{constant}$, and arguments precisely similar to those leading to (12) give for these components the results

$$\omega_x = (A \sin \lambda) v_x \frac{\partial t}{\partial \rho_0}, \qquad \omega_\rho = (A \sin \lambda) \left(v_\rho \frac{\partial t}{\partial \rho_0} - \frac{\partial \rho}{\partial \rho_0} \right). \tag{49}$$

Accordingly, the secondary trailing vorticity is

$$\lim_{x \to +\infty} (\omega_x) = (A \sin \lambda) X'(\rho). \tag{50}$$

Since, as (46) shows, t is necessarily calculated in the first place as a function $t(x, \rho_0)$, the formulas (49) in terms of that function will be found most convenient for practical application in § 7. It is interesting and instructive, however, by analogy with § 4, to see what they become in terms of a t which, once calculated, is expressed as a function of x and ρ, rather than of x and ρ_0. From (45) and the expressions for the velocity components in terms of Stokes's stream function,

$$\frac{\partial\rho_0}{\partial x}=-\left(\frac{\rho}{\rho_0}\right)\frac{v_\rho}{U},\qquad \frac{\partial\rho_0}{\partial\rho}=\left(\frac{\rho}{\rho_0}\right)\frac{v_x}{U}. \tag{51}$$

Using these results to transform (49) for the case when t is expressed as a function $t(x,\rho)$, we obtain

$$\omega_x=(A\sin\lambda)U\frac{\rho_0}{\rho}\frac{\partial t}{\partial\rho},\qquad \omega_\rho=-(A\sin\lambda)U\frac{\rho_0}{\rho}\frac{\partial t}{\partial x}. \tag{52}$$

Thus the vorticity resultant in each meridian plane, while perpendicular to grad t as in §4, is proportional in magnitude to (ρ_0/ρ) grad t. This, like the corresponding two-dimensional result, can alternatively be derived from conservation of mass. The mass of fluid in an annular region bounded by two neighbouring axisymmetrical streamtubes and by two neighbouring surfaces $t=$ constant is proportional to the product of the radius ρ, the distance between the two surfaces $t=$ constant, and the length of an element in which the part of a surface $t=$ constant between the two streamtubes is cut by a meridian plane. For this product to remain constant along a streamline, the length of such an element must vary as (grad t)/ρ, whence the required result follows.

The author could not obtain by inspection the velocity field corresponding to the values of ω_λ, ω_x and ω_ρ given by (48) and (52); a field whose curl is as required is fairly easily found, but it is not solenoidal, nor does it satisfy the boundary conditions! Therefore, the direct use of the Biot–Savart formula for calculating the secondary velocity field seems to be necessary.

Finally, it may be noted that in some problems it is convenient to use the spherical polar coordinates r, θ, where

$$r\cos\theta=x,\qquad r\sin\theta=\rho, \tag{53}$$

instead of x and ρ. The 'longitude' λ is retained. By considering the stretching of a vortex element joining streamlines specified by (ρ_0,λ) and $(\rho_0+\delta\rho_0,\lambda)$ we obtain (exactly as (8) was obtained) the equations

$$\omega_r=(-A\sin\lambda)\left(\frac{\partial r}{\partial\rho_0}\right)_{t,\lambda},\qquad \omega_\theta=(-A\sin\lambda)\left(r\frac{\partial\theta}{\partial\rho_0}\right)_{t,\lambda}, \tag{54}$$

where equation (47) for the initial vorticity of the element has been used. If the time is expressed as $t(\rho_0, r)$, then

$$\left(\frac{\partial r}{\partial\rho_0}\right)_{t,\lambda}=-\frac{\partial t/\partial\rho_0}{\partial t/\partial r}=-v_r\frac{\partial t}{\partial\rho_0},\qquad \left(r\frac{\partial\theta}{\partial\rho_0}\right)_{t,\lambda}=\left(r\frac{\partial\theta}{\partial\rho_0}\right)_{r,\lambda}+\frac{v_\theta}{v_r}\left(\frac{\partial r}{\partial\rho_0}\right)_{t,\lambda}, \tag{55}$$

as in (10) and (11), giving

$$\omega_r=(A\sin\lambda)v_r\frac{\partial t}{\partial\rho_0},\qquad \omega_\theta=(A\sin\lambda)\left(v_\theta\frac{\partial t}{\partial\rho_0}-r\frac{\partial\theta}{\partial\rho_0}\right), \tag{56}$$

where r, λ are kept constant in the differentiations. If, alternatively, the time is expressed as $t\ (\rho_0,\theta)$, then

$$\left(r\frac{\partial\theta}{\partial\rho_0}\right)_{t,\lambda}=-\frac{\partial t/\partial\rho_0}{\partial t/r\partial\theta}=-v_\theta\frac{\partial t}{\partial\rho_0},\qquad \left(\frac{\partial r}{\partial\rho_0}\right)_{t,\lambda}=\left(\frac{\partial r}{\partial\rho_0}\right)_{\theta,\lambda}+\frac{v_r}{v_\theta}\left(r\frac{\partial\theta}{\partial\rho_0}\right)_{t,\lambda}, \tag{57}$$

giving
$$\omega_\theta = (A\sin\lambda) v_\theta \frac{\partial t}{\partial \rho_0}, \qquad \omega_r = (A\sin\lambda)\left(v_r \frac{\partial t}{\partial \rho_0} - \frac{\partial r}{\partial \rho_0}\right), \tag{58}$$
where θ, λ are kept constant in the differentiations. If, lastly, the time is expressed as $t(r,\theta)$, then the sentence following equation (52) makes it clear that
$$\omega_r = (A\sin\lambda) U \frac{\rho_0}{\rho} \frac{1}{r} \frac{\partial t}{\partial \theta}, \qquad \omega_\theta = -(A\sin\lambda) U \frac{\rho_0}{\rho} \frac{\partial t}{\partial r}. \tag{59}$$

6. Evaluation of t for flow past a sphere

The drift function t will now be studied in detail for flow past a sphere, principally so that the results can be substituted in the formulas of §§2, 3 and 5, and the secondary flow evaluated.

Spherical polar coordinates r, θ, λ are used. From Stokes's stream function for flow past a sphere, and equation (45), the streamlines are given by
$$\rho_0^2 = r^2 \sin^2\theta \left(1 - \frac{a^3}{r^3}\right), \tag{60}$$
where a is the radius of the sphere. Two alternative equations for obtaining the time t are useful in different regions, namely
$$dt = \frac{dr}{v_r} = \frac{dr}{U\left(1 - \dfrac{a^3}{r^3}\right)\cos\theta}, \tag{61}$$
and
$$dt = \frac{r d\theta}{v_\theta} = -\frac{r d\theta}{U\left(1 + \dfrac{a^3}{2r^3}\right)\sin\theta} \tag{62}$$
On any given streamline, by (1),
$$t + r/U \to 0 \quad \text{as } \theta \to \pi, \tag{63}$$
since $x + r \to 0$. The integral for t derivable from (60), (61) and (63) is unfortunately hyperelliptic, as Darwin (1953) points out. However, valuable expansions of it can be obtained both for large and small values of ρ_0/a.

For large ρ_0/a, the solution for r of equation (60) can be expanded in powers of a^3/ρ_0^3 as
$$r = \frac{\rho_0}{\sin\theta}\left(1 + \frac{1}{2}\frac{a^3}{\rho_0^3}\sin^3\theta - \frac{3}{8}\frac{a^6}{\rho_0^6}\sin^6\theta + \dots\right). \tag{64}$$
It follows that (62) can be expanded as
$$\begin{aligned} U dt &= -\frac{\rho_0 d\theta}{\sin^2\theta} \frac{\left(1 - \dfrac{a^3}{r^3}\right)^{-1/2}}{1 + \dfrac{a^3}{2r^3}} \\ &= -\frac{\rho_0 d\theta}{\sin^2\theta}\left\{1 + \frac{\dfrac{3}{8}\dfrac{a^6}{r^6} + \dfrac{5}{16}\dfrac{a^9}{r^9} + \dfrac{35}{128}\dfrac{a^{12}}{r^{12}} + \dots}{1 + \dfrac{a^3}{2r^3}}\right\} \\ &= -\frac{\rho_0 d\theta}{\sin^2\theta}\left(1 + \frac{3}{8}\frac{a^6}{\rho_0^6}\sin^6\theta - \frac{a^9}{\rho_0^9}\sin^9\theta + \frac{315}{128}\frac{a^{12}}{\rho_0^{12}}\sin^{12}\theta + \dots\right). \end{aligned} \tag{65}$$

Integrating,

$$Ut=\rho_0\cot\theta+\frac{3}{8}\frac{a^6}{\rho_0^5}\int_\theta^\pi \sin^4\theta\,d\theta-\frac{a^9}{\rho_0^8}\int_\theta^\pi \sin^7\theta\,d\theta+\frac{315}{128}\frac{a^{12}}{\rho_0^{11}}\int_\theta^\pi \sin^{10}\theta\,d\theta-\ldots, \tag{66}$$

where the integrals have been made definite in such a way that (63) is satisfied.

The radius of convergence of the series (65) is easily determined from the position of the singularities of $r/(1+a^3/2r^3)$ as a function of $\rho_0\operatorname{cosec}\theta$. The series converges for $\rho_0>3^{1/2}2^{-1/3}a\sin\theta$. Hence (66) converges for all θ provided that $\rho_0/a>3^{1/2}2^{-1/3}=1{\cdot}375$*.

Darwin's drift distance is inferred from (66) as

$$\begin{aligned}X(\rho_0)\lim_{x\to+\infty}(Ut-x)&=\frac{3}{8}\frac{a^6}{\rho_0^5}\left(\frac{3\pi}{8}\right)-\frac{a^9}{\rho_0^8}\left(\frac{32}{35}\right)+\frac{315}{128}\frac{a^{12}}{\rho_0^{11}}\left(\frac{63\pi}{256}\right)-\ldots\\&=0{\cdot}442\frac{a^6}{\rho_0^5}-0{\cdot}914\frac{a^9}{\rho_0^8}+1{\cdot}903\frac{a^{12}}{\rho_0^{11}}-\ldots,\end{aligned} \tag{67}$$

the fractions in brackets being the values of the integrals in (66) for $\theta=0$.

Note that (66) has the properties (obviously true on any streamline from the symmetry of the flow)

$$\left.\begin{aligned}t(\theta)-t(\tfrac{1}{2}\pi)&=t(\tfrac{1}{2}\pi)-t(\pi-\theta),\\X(\rho_0)=\lim_{\theta\to0}(Ut-x)&=2(Ut)_{\theta=\pi/2}-\lim_{\theta\to\pi}(Ut-x)=2(Ut)_{\theta=\pi/2}.\end{aligned}\right\} \tag{68}$$

For small ρ_0/a, each streamline (60) is divided into two parts, one on which θ is near 0 or π (that is, $\sin\theta$ is small) and one on which $(r-a)/a$ is small. When θ is near π, we use the approximation

$$-\sec\theta \doteqdot 1+\tfrac{1}{2}\sin^2\theta \tag{69}$$

in (61), together with (60) and (63), to obtain

$$\begin{aligned}Ut&=-r+\int_r^\infty\left\{\frac{1}{1-a^3/r^3}+\frac{1}{2}\frac{\rho_0}{r^2}\frac{1}{(1-a^3/r^3)^2}-1\right\}dr\\&=-r+\frac{1}{6}\frac{\rho_0^2r^3}{r^3-a^3}-\frac{1}{3}a\left(1+\frac{\rho_0^2}{3a^2}\right)\log\frac{r-a}{\sqrt{(r^2+ar+a^2)}}\\&\qquad-\frac{1}{\sqrt{3}}a\left(1-\frac{\rho_0^2}{3a^2}\right)\tan^{-1}\left(\frac{a\sqrt{3}}{a+2r}\right).\end{aligned} \tag{70}$$

We suppose that this approximation is valid down to $r=r_0$ (say), after which θ departs too greatly from π but $(r-a)/a$ is small. For $r<r_0$, we use (62) with the approximation

$$\frac{r}{1+\dfrac{a^3}{2r^3}}\doteqdot\frac{2}{3}a+\frac{4}{3}(r-a)\doteqdot\frac{2}{3}a+\frac{4}{9}\frac{\rho_0^2}{a}\operatorname{cosec}^2\theta \tag{71}$$

* Some improvement in convergence arises if the series (66) is rearranged as a series in powers of a/r (with coefficients functions of θ), using (64). This has not been done, however, because of the desirability of knowing t as a function of ρ_0 for the application of the results of §5. The results it gives for $X(\rho)$ are identical with those obtained by the method used below.

(in which the error is of the order ρ_0^4) to obtain

$$Ut = \frac{1}{2}X(\rho_0) + \frac{2}{3}a\left(1+\frac{\rho_0^2}{3a^2}\right)\log\cot\tfrac{1}{2}\theta + \frac{2\rho_0^2}{9a}\cot\theta\,\mathrm{cosec}\,\theta. \tag{72}$$

where the arbitrary constant is determined by putting $\theta = \frac{1}{2}\pi$ and using (68). Comparing (70) and (72) for values of r and θ for which both approximations are valid (and also (60) holds), we obtain after some calculation

$$X(\rho_0) = \frac{4}{3}a\left(1+\frac{\rho_0^2}{3a^2}\right)\log\frac{3^{3/4}(2a)}{\rho_0} - \left(2+\frac{\pi}{3\sqrt{3}}\right)a + \left(\frac{\pi}{\sqrt{3}}-1\right)\frac{\rho_0^2}{9a}. \tag{73}$$

As Darwin points out, $X(\rho_0)$ is logarithmically infinite at $\rho_0 = 0$. This is because there is an infinite time-delay as fluid approaches any stagnation point where the tangent to the body surface is smoothly-turning.

In figure 2, the function $\rho X(\rho)/a^2$ is plotted against ρ/a, the expression (73) being used for $\rho/a \leqslant 0{\cdot}4$, and expression (67) for $\rho/a \geqslant 1{\cdot}5$ (some allowance for the later terms in the series being made up in this case by assuming that the coefficients remain in approximate geometrical progression). To interpolate between them we use Darwin's result (14) to give

$$\int_0^\infty \frac{\rho X(\rho)}{a^2}\,d\left(\frac{\rho}{a}\right) = \frac{1}{2\pi a^3}\int_{-\infty}^{\infty}\int_{-\infty}^{\infty} X(y,z)\,dy\,dz = \frac{1}{2\pi a^3}\left(\frac{2}{3}\pi a^3\right) = \frac{1}{3}, \tag{74}$$

since the hydrodynamic mass of a sphere is half the displaced mass of fluid. Practically no choice is possible if a smooth interpolation between the two crosses in figure 2 is to be made which satisfies (74), and a 'French curve' has been selected and used for this purpose which makes the integral from $0{\cdot}4$ to $1{\cdot}5$ (calculated by Simpson's rule) make up exactly for the amount by which the sum of the (analytically evaluated) integrals from 0 to $0{\cdot}4$ and $1{\cdot}5$ to ∞ falls short of $\frac{1}{3}$. The values of $X(\rho)/a$ itself as a function of ρ/a have been read off figure 2 and are presented in figure 3 and table 1.

Once $X(\rho)$ has been obtained, it is a simple matter to compute the function t throughout the field. For $\theta > \frac{5}{6}\pi$, (69) is a good approximation, and accordingly the formula (70) has been used for t. For $\frac{1}{2}\pi < \theta < \frac{5}{6}\pi$, two formulas have been used: when $r/a < 1{\cdot}5$, (71) is a good approximation, and

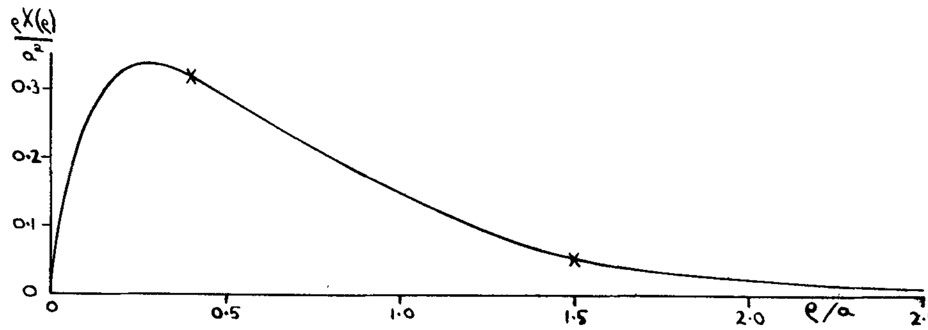

Figure 2. The method of interpolation used to derive Darwin's 'total drift' function X(ρ) for irrotational flow past a sphere.

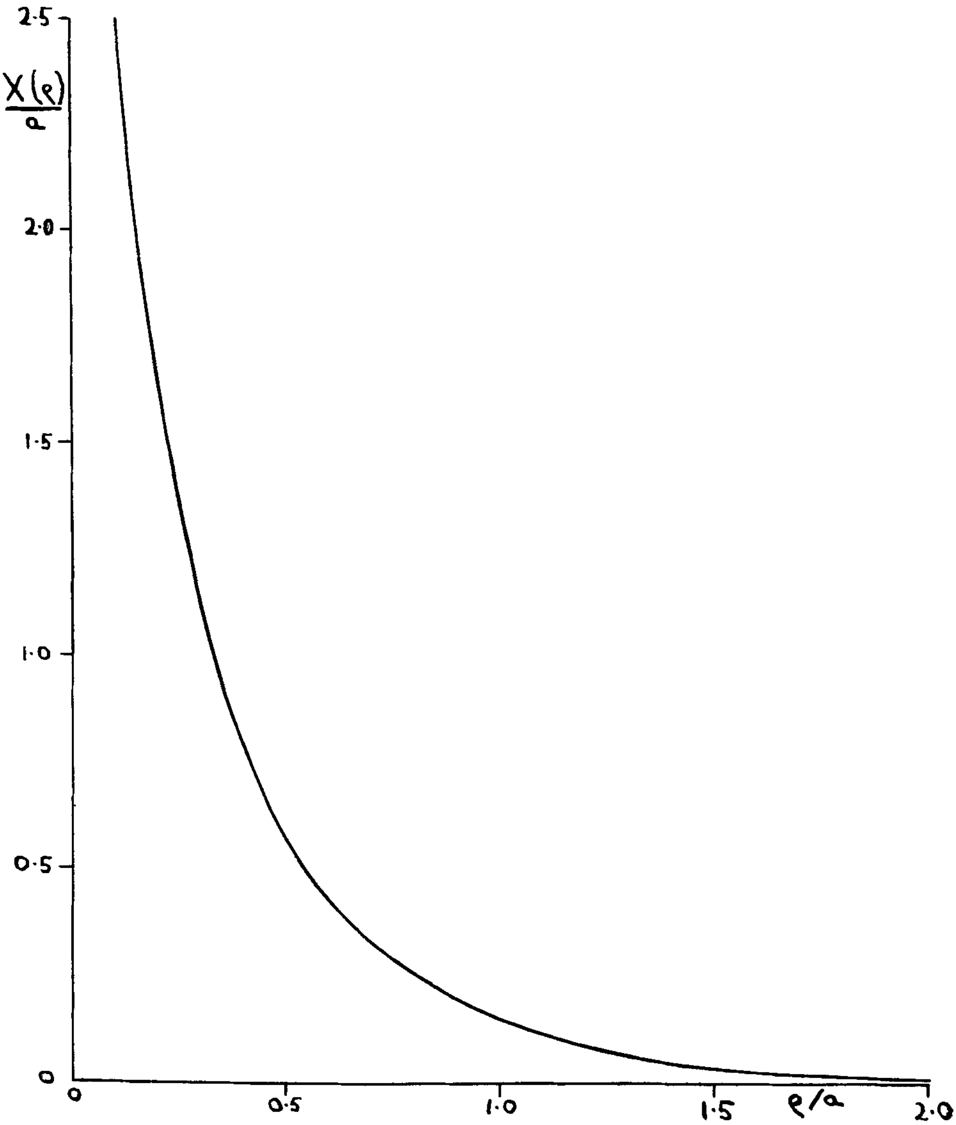

Figure 3. Darwin's 'total drift' function $X(\rho)$ for irrotational flow past a sphere. Since the scales used for ρ and $X(\rho)$ are the same, the figure gives the actual shape into which planes of fluid, initially at right angles to the stream, would ultimately be distorted in such a flow.

ρ/a	0·05	0·1	0·15	0·2	0·25	0·3	0·35	0·4
$X(\rho)/a$	3·418	2·504	1·980	1·616	1·340	1·124	0·947	0·799
ρ/a	0·5	0·6	0·7	0·8	0·9	1·0	1·1	1·2
$X(\rho)/a$	0·576	0·430	0·327	0·252	2·194	0·150	0·115	0·087
ρ/a	1·3	1·4	1·5	1·75	2·0	2·25	2·5	
$X(\rho)/a$	0·065	0·048	0·036	0·020	0·011	0·007	0·004	

Table 1.

so formula (72) has been used for t, while when $r/a > 1{\cdot}75$, we have $\rho_0 \operatorname{cosec} \theta > 1{\cdot}58\,a$, which is well inside the radius of convergence of (65), so that (66) has been used. The interpolation across the small gap is straightforward. For $\theta < \frac{1}{2}\pi$, equation (68) has been used to deduce t from its values when $\theta > \frac{1}{2}\pi$. The results are exhibited in figure 4, where the surfaces $t = \text{constant}$ are shown for values of Ut/a proceeding by intervals of 0·5 from $-2{\cdot}5$ to $+3$. The streamlines $\rho_0/a = 0{\cdot}125, 0{\cdot}25, 0{\cdot}375, 0{\cdot}5, 0{\cdot}75, 1{\cdot}0, 1{\cdot}5$ and 2·5 are also shown.

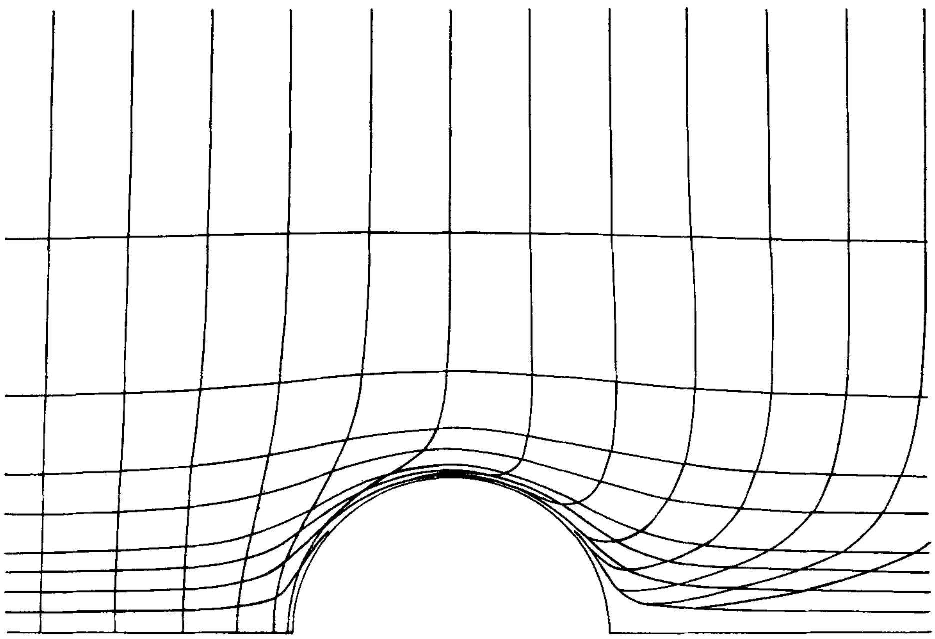

Figure 4. The irrotational flow past a sphere : streamlines and surfaces $t = \text{constant}$. The latter are the shapes into which planes of fluid initially at right angles to the stream would be distorted as they passed over the sphere (if the flow were irrotational).

Figure 4 has two uses. First, it exhibits a steady fluid motion in far more detail than has ever been given before, showing precisely what happens to every particle of fluid and *when* (Darwin's figure 1, representing flow past a circular cylinder, is insufficiently detailed for this purpose.) Secondly, in the problem of shear flow past a sphere, it exhibits precisely how vortex elements initially in the ρ-direction are stretched and change their direction during passage of the sphere. An impression of the values of the vorticity resultant in a meridian plane can be derived either by observing this stretching, or by means of the rule derived in § 5 that along any streamline the product of this vorticity with the distance from the axis varies inversely as the distance between successive surfaces $t = \text{constant}$. Numerical values of the vorticity components are obtained in § 7.

An alternative mode of display of the function t is adopted in figure 5, which shows the variation of Ut/a along all but one of the streamlines in figure 4, by plotting Ut/a as a function of $x = r\cos\theta$ for each value of ρ_0/a. A third manner of representation of some of the results (figure 6) will be discussed in § 7.

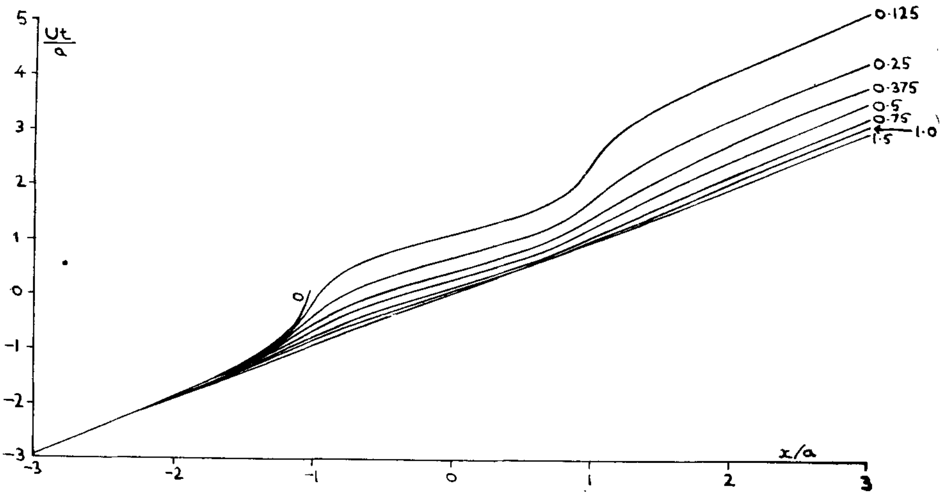

Figure 5. Variation of the drift function t, for flow past a sphere of radius a, along different streamlines, which are identified on the figure by the values of ρ_0/a noted on each curve. Here, ρ_0 is the distance of a streamline from the axis far upstream.

7. The vorticity field in weakly-sheared flow past a sphere

The drift function t having been evaluated for irrotational flow past a sphere, equations (56) and (58) show that only its derivative with respect to ρ_0 (keeping either r or θ constant) is needed to deduce both ω_r and ω_θ in the problem of weakly-sheared flow past a sphere.

In the region $\theta > \frac{5}{6}\pi$, where t has been expressed as a function of ρ_0 and r as in (70), equations (56) are applicable; in applying them, we note that by (60)

$$r\left(\frac{\partial\theta}{\partial\rho_0}\right)_r = \frac{r\tan\theta}{\rho_0}. \tag{75}$$

In the region $\frac{1}{2}\pi < \theta < \frac{5}{6}\pi$, where t has been expressed as two different functions of ρ_0 and θ in different ranges of ρ_0, the detailed computations of t were done for $\theta = 90°(10°)150°$, with a suitable selection of values of ρ_0 in each case; a small gap is present ($1{\cdot}5 < r/a < 1{\cdot}75$) where neither formula is reliable. However, as figure 6 shows, a smooth curve can easily be drawn through the points which are available for each θ. From these $(\partial t/\partial\rho_0)_\theta$ can be inferred by measuring the slope of the curve; for the larger and smaller values of ρ_0/a, however, analytical differentiation is preferable. The resulting tables of values can then be improved by the technique of

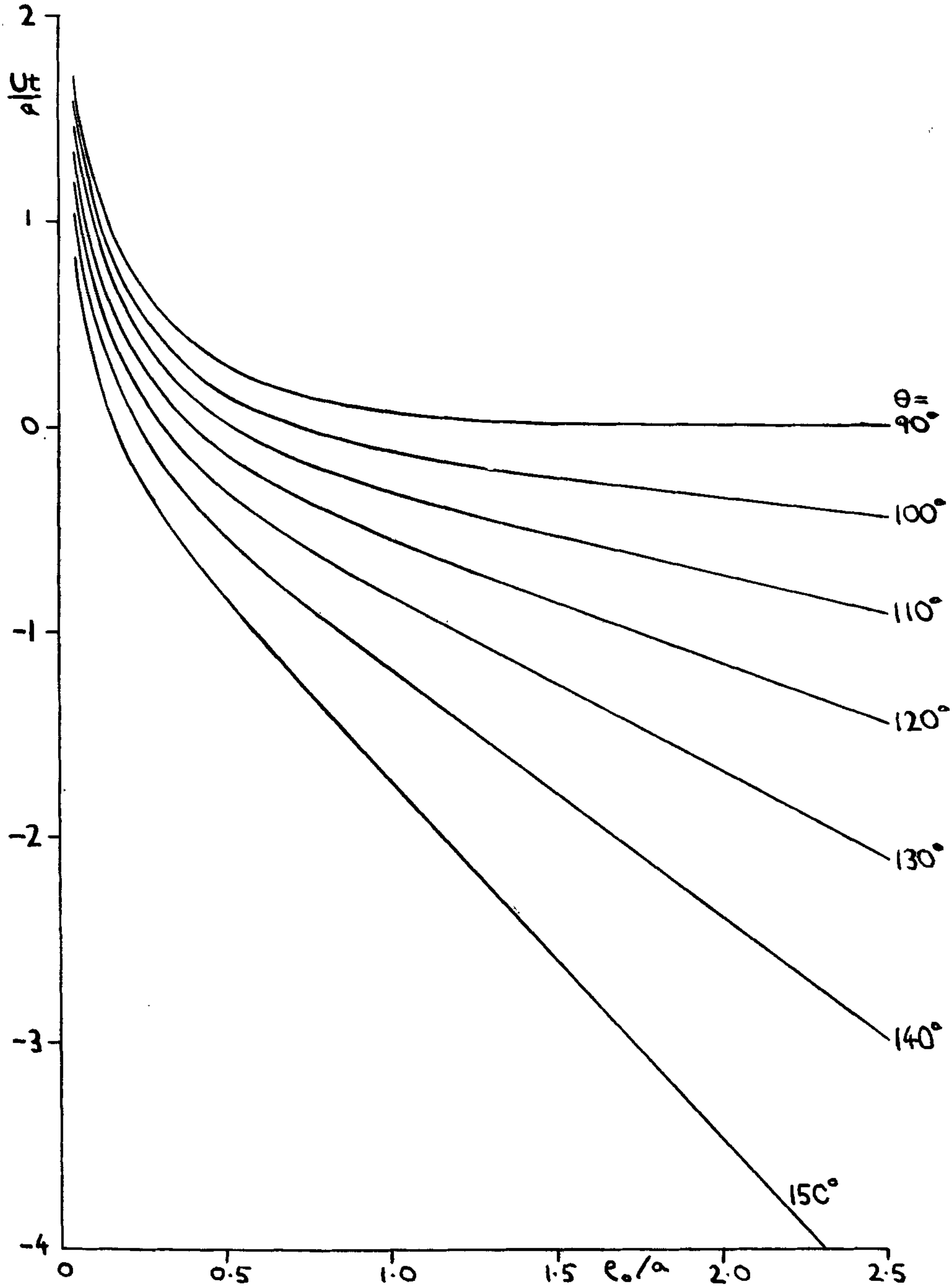

Figure 6. Variation of the drift function t with ρ_0 for constant values of the spherical polar coordinate θ.

'graduation', or smoothing of data. When this has been done, ω_r and ω_θ are inferred from (58), in which, by (60),

$$\left(\frac{\partial r}{\partial \rho_0}\right)_\theta = \frac{r(r^3-a^3)}{\rho_0(r^3+\frac{1}{2}a^3)}. \tag{76}$$

The same technique applied to the values of $X(\rho)$ itself gives the important function $X'(\rho)$, which by (50) determines the secondary trailing vorticity distribution. Since $X'(\rho) \to \infty$ as $\rho \to 0$, it is convenient to exhibit the product $-\rho X'(\rho)$ in Table 2. Certain of the values can be compared with

ρ/a	0	0·05	0·1	0·15	0·2	0·25	0·3	0·35
$-\rho X'(\rho)/a$	1·333	1·325	1·307	1·283	1·253	1·214	1·166	1·112
ρ/a	0·4	0·5	0·6	0·7	0·8	0·9	1·0	1·1
$-\rho X'(\rho)/a$	1·043	0·897	0·749	0·621	0·523	0·450	0·394	0·345
ρ/a	1·2	1·3	1·4	1·5	1·75	2·0	2·25	2·5
$-\rho X'(\rho)/a$	0·298	0·249	0·198	0·151	0·079	0·049	0·030	0·019

Table 2.

results for the secondary trailing vorticity given by Hawthorne & Martin (1955), who obtain values of $(\omega_x)_{x=+\infty}/A\sin\lambda$ equal to 12·976, 4·792, 1·852 and 0·404 for $\rho_0/a=0{\cdot}1$, 0·25, 0·5 and 1·0 respectively. These values, obtained by numerical integration along streamlines, differ from those to be obtained from Table 2 (by dividing by ρ/a) by $-0{\cdot}09$, $-0{\cdot}06$, $+0{\cdot}06$ and $+0{\cdot}01$ respectively. Errors in both methods probably contribute about equally to these discrepancies, although in the case $\rho/a=0{\cdot}1$ the value in Table 2, based on expression (73) for small ρ/a, can perhaps be preferred*.

The general distribution of vorticity is shown in Table 3, where the variation of ω_{1r} and $\omega_{1\theta}$ along three particular streamlines $\rho_0/a=\frac{1}{4}$, $\frac{1}{2}$ and 1 is exhibited by giving their values at 10° intervals of the polar angle θ. These streamlines were selected partly because they give a good general idea of the variation of ω_{1r} and $\omega_{1\theta}$ over the field of flow, and partly because they give a convenient basis (as will be seen in a later paper) for the evaluation of the Biot–Savart field of $\boldsymbol{\omega}_1$, by integration first with respect to λ, secondly with respect to θ along a streamline $\rho_0=$ constant, and finally with respect to ρ_0. The vorticity change $\boldsymbol{\omega}_1$ is tabulated as being the quantity directly responsible for the secondary flow. The absolute vorticity components ω_r and ω_θ can, however, be obtained by adding to ω_{1r} and $\omega_{1\theta}$ the values of the undisturbed vorticity components ($\omega_r=-A\sin\lambda\sin\theta$, $\omega_\theta=-A\sin\lambda\cos\theta$) which are tabulated on the left.

Professor Hawthorne has kindly supplied the author with the results of computations, additional to those given in Hawthorne & Martin (1955), from which values of ω_{1r} and $\omega_{1\theta}$ can be deduced. Comparisons with the values to Table 3 at a sample of points show agreement to within the same order of accuracy as was noted above for the secondary trailing vorticity.

* $-\rho X'(\rho)/a$ is given as a series of powers of $(\rho/a)^2$ of which the first two terms for $\rho/a=0{\cdot}1$ are $1{\cdot}333-0{\cdot}026$; the next would be expected to be less than 0·001.

Values of the vorticity change $\boldsymbol{\omega}_1$ and of r/a along three particular streamlines.

	Undisturbed values of		Values for $\rho_0/a=\frac{1}{4}$			Values for $\rho_0/a=\frac{1}{2}$			Values for $\rho_0/a=1$		
	$\frac{\omega_r}{A\sin\lambda}$	$\frac{\omega_\theta}{A\sin\lambda}$	$\frac{\omega_{1r}}{A\sin\lambda}$	$\frac{\omega_{1\theta}}{A\sin\lambda}$	r/a	$\frac{\omega_{1r}}{A\sin\lambda}$	$\frac{\omega_{1\theta}}{A\sin\lambda}$	r/a	$\frac{\omega_{1r}}{A\sin\lambda}$	$\frac{\omega_{1\theta}}{A\sin\lambda}$	r/a
0°	0	−1·000	−4·86	0	∞	−1·79	0	∞	−0·39	0	∞
10°	−0·174	−0·985	−3·65	0·80	1·638	−1·67	$0{\cdot}29_7$	2·938	−0·38	$0{\cdot}06_5$	5·774
20°	−0·342	−0·940	−1·55	1·57	1·177	−1·23	0·54	1·655	−0·34	0·12	2·981
30°	−0·500	−0·866	−0·51	2·20	1·083	−0·66	0·76	1·325	−0·25	0·16	2·115
40°	−0·643	−0·766	+0·02	2·71	1·050	−0·21	0·94	1·200	−0·13	0·19	1·731
50°	−0·766	−0·643	0·34	3·11	1·035	+0·12	1·09	1·141	+0·02	0·21	1·535
60°	−0·866	−0·500	0·56	3·41	1·028	0·35	1·22	1·111	0·15	0·23	1·426
70°	−0·940	−0·342	0·70	3·58	1·024	0·51	1·28	1·094	0·26	0·24	1·366
80°	−0·985	−0·174	0·79	3·63	1·021	0·61	1·28	1·086	0·34	0·24	1·334
90°	−1·000	0	0·83	3·57	1·021	0·67	1·25	1·083	0·38	0·24	1·325
100°	−0·985	0·174	0·84	3·41	1·021	0·68	1·17	1·086	0·38	0·23	1·334
110°	−0·940	0·342	0·81	3·12	1·024	0·65	1·05	1·094	0·34	0·20	1·366
120°	−0·866	0·500	0·75	2·74	1·028	0·59	0·90	1·111	0·29	0·17	1·426
130°	−0·766	0·643	0·65	2·29	1·035	0·49	0·74	1·141	0·20	0·13	1·535
140°	−0·643	0·766	0·53	1·76	1·050	0·37	0·55	1·200	0·11	0·08	1·731
150°	−0·500	0·866	0·39	1·20	1·083	0·23	0·32	1·325	0·05	0·05	2·115
160°	−0·342	0·940	0·22	0·62	1·177	0·09	0·14	1·655	0·01	$0{\cdot}01_8$	2·981
170°	−0·174	0·985	0·04	0·14	1·638	$0{\cdot}00_7$	$0{\cdot}02_0$	2·938	$0{\cdot}00_{09}$	$0{\cdot}00_{26}$	5·774
180°	0	1·000	0	0	∞	0	0	∞	0	0	∞

Table 3.

For values of ρ_0/a which are either large or small, the direct use of equations (56) and (58), with the approximation (66) or (70) or (72) for t, is recommended in preference to the numerical procedures described above. Here, to save space, we give only the *first* approximation to ω_{1r} and $\omega_{1\theta}$ in each case. For large r/a, except immediately downstream of the sphere,

$$\omega_{1r} \sim A \sin\lambda \sin\theta \left(\frac{a}{r}\right)^3, \qquad \omega_{1\theta} \sim -\tfrac{1}{2}A \sin\lambda \cos\theta \left(\frac{a}{r}\right)^3. \tag{77}$$

For θ near π,

$$\left.\begin{aligned} \omega_{1r} &\sim A \sin\lambda \sin\theta \left\{1 - \frac{1}{3}\left(1 - \frac{a^3}{r^3}\right)^{1/2} - \frac{2r}{9a}\left(1 - \frac{a^3}{r^3}\right)^{3/2} \right. \\ &\qquad \left. \times \left[\log \frac{\sqrt{(r^2+ar+a^2)}}{r-a} + (\sqrt{3})\tan^{-1}\left(\frac{a\sqrt{3}}{a+2r}\right)\right]\right\}, \\ \omega_{1\theta} &\sim A \sin\lambda \cos\theta \left\{1 - \left(1 - \frac{a^3}{r^3}\right)^{-1/2}\right\}. \end{aligned}\right\} \tag{78}$$

For θ near 0, we must add on to the values (78) the considerably larger values

$$\left.\begin{aligned} \omega_{1r} &\sim A \sin\lambda \cos\theta \left(1 - \frac{a^3}{r^3}\right) X'(\rho_0), \\ \omega_{1\theta} &\sim -A \sin\lambda \sin\theta \left(1 + \frac{a^3}{2r^3}\right) X'(\rho_0). \end{aligned}\right\} \tag{79}$$

For small $(r-a)/a$,

$$\omega_{1r} \sim A \sin\lambda \sin\theta, \qquad \omega_{1\theta} \sim A \sin\lambda \left(1 - \frac{a^3}{r^3}\right)^{-1/2}. \tag{80}$$

Finally, we note the simple exact form of the third component ω_λ of the secondary vorticity, which by (48) and (60) is

$$\omega_\lambda = -A \cos\lambda \left(1 - \frac{a^3}{r^3}\right)^{-1/2}, \qquad \omega_{1\lambda} = A \cos\lambda \left\{1 - \left(1 - \frac{a^3}{r^3}\right)^{-1/2}\right\}. \tag{81}$$

It is interesting that this component shows no dependence on θ.

References

Darwin, C. G. 1953 *Proc. Camb. Phil. Soc.* **49**, 342.

Hawthorne, W. R. 1951 *Proc. Roy. Soc.* A, **206**, 374.

Hawthorne, W. R. 1954 *J. Aero. Sci.* **21**, 588.

Hawthorne, W. R. & Martin, Moira E. 1955 *Proc. Roy. Soc.* A, **232**, 184.

Lighthill, M. J. 1956 *Proc. Camb. Phil. Soc.* **52**, 317.

Taylor, G. I. 1928 *Proc. Roy. Soc.* A, **120**, 13.

Young, A. D. & Maas, J. N. 1936 *Aero. Res. Counc., Lond., Rep. & Mem.* no. 1770.